Evaporating loop quantum black hole

Leonardo Modesto*

Department of Physics, Bologna University & INFN Bologna,
V. Irnerio 46, I-40126 Bologna, EU.
Centre de Physique Théorique de Luminy, Université de la Méditerranée,
Case 907, F-13288 Marseille, EU.

Abstract

In this paper we obtain the black hole metric from a semiclassical analysis of loop quantum black hole. Our solution and the Schwarzschild one tend to match well at large distances from Planck region. In $r = 0$ the semiclassical metric is regular and singularity free in contrast to the classical one. By using the new metric we calculate the Hawking temperature and the entropy. For the entropy we obtain the logarithmic correction to the classical area law. Finally we study the mass evaporation process and we show the mass and temperature tend to zero at infinitive time.

Introduction

Quantum gravity is the theory by which we tray to reconcile general relativity and quantum mechanics. In general relativity the space-time is dynamical then it is not possible to study other interactions on a fixed background because the background itself is a dynamical field. The theory called "loop quantum gravity" (LQG) [1] is the most widespread nowadays. This is one of the non perturbative and background independent approaches to quantum gravity (another non perturbative approach to quantum gravity is called "asymptotic safety quantum gravity" [2]). Loop quantum gravity is a quantum geometric fundamental theory that reconciles general relativity and quantum mechanics at the Planck scale. The main problem nowadays is to connect this fundamental theory with standard model of particle physics and in particular with the effective quantum field theory. In the last two years great progresses has been done to connect (LQG) with the low energy physics by the general boundary approach [3], [4]. Using this formalism it has been possible to calculate the graviton propagator in four [5], [6] and three dimensions [7], [8]. In three dimensions it has been showed that a noncommuative field theory can be obtained from spinfoam models [9]. Similar efforts in four dimension are going in progress [10].

Early universe and black holes are other interesting places for testing the validity of LQG. In the past years applications of LQG ideas to minisuperspace models lead to some interesting results in those fields. In particular it has been showed in cosmology [11], [12] and recently in black hole physics [13], [14], [15], [16] that it is possible to solve the cosmological singularity problem and the black hole singularity problem by using tools and ideas developed in full loop quantum gravity theory.

*Electronic address: modesto@bo.infn.it or leonardo.modesto@virgilio.it

We can summarize this short introduction to "loop quantum gravity program" in two research lines; the first one dedicated to obtain quantum field theory from the fundamental theory and the other one dedicated to apply LQG to cosmology and astrophysical objects where extreme energy conditions need to know a quantum gravity theory.

In this paper we concentrate our attention on the second research line. We study the black hole physics using ideas suggested by loop quantum gravity at the semiclassical level (by "loop quantum black hole" [16], extending the metric of obtained [17] to all space-time). The new metric is regular in $r = 0$ where the classical singularity is localized and we are interesting to calculate the temperature, entropy and to analyze the evaporation process.

This paper is organized in two section as follows. In the first section we briefly recall the semiclassical Schwarzschild solution inside the black hole [17] and we extend the solution outside the event horizon showing the regularity of the curvature invariant $\forall\, r \geqslant 0$. In the second section we calculate the Hawking temperature and the entropy in terms of the event horizon area. In the same section we study also the mass evaporation process discussing the new physics suggested by loop quantum gravity.

1 Semiclassical black hole solution

In this section we summarize the solution calculated in paper [17] and we extend the solution to all the space-time. We start to study the region inside the event horizon where the Ashtekar's connection and density triad are

$$
\begin{aligned}
A &= c\tau_3 dx + b\tau_2 d\theta - b\tau_1 \sin\theta d\phi + \tau_3 \cos\theta d\phi, \\
E &= p_c \tau_3 \sin\theta \frac{\partial}{\partial x} + p_b \tau_2 \sin\theta \frac{\partial}{\partial \theta} - p_b \tau_1 \frac{\partial}{\partial \phi},
\end{aligned} \tag{1}
$$

(where $\tau_i = -\frac{i}{2}\sigma_i$ and σ_i are the Pauli matrices). The variables in the phase space are: (b, p_b), (c, p_c), and the Poisson algebra is: $\{c, p_c\} = 2\gamma G_N$, $\{b, p_b\} = \gamma G_N$. The Hamiltonian constraint of "loop quantum black hole" [16] in terms of holonomies [1] depends explicitly on the parameter δ that defines the length of the curves along which we integrate the connections. The parameter δ is not an external cutoff but instead a result of full loop quantum gravity [18]. The Hamiltonian constraint $\mathcal{C}^\delta$ in (2) can be substantially simplified in the particular gauge $N = \frac{\gamma \sqrt{|p_c|}\mathrm{sgn}(p_c)\delta^2}{16\pi G_N \sin\delta b}$

$$
\mathcal{C}^\delta = -\frac{1}{2\gamma G_N}\Big\{2\sin\delta c\; p_c + \Big(\sin\delta b + \frac{\gamma^2\delta^2}{\sin\delta b}\Big)p_b\Big\}. \tag{4}
$$

[1] The Hamiltonian constraint in terms of holonomies is

$$
\begin{aligned}
\mathcal{C}^\delta &= -\frac{2\hbar N}{\gamma^3\delta^3 l_P^2}\mathrm{Tr}\left(\sum_{ijk}\epsilon^{ijk} h_i^{(\delta)} h_j^{(\delta)} h_i^{(\delta)-1} h_k^{(\delta)}\left\{h_k^{(\delta)-1}, V\right\} + 2\gamma^2\delta^2\tau_3 h_1^{(\delta)}\left\{h_1^{(\delta)-1}, V\right\}\right) = \\
&= -\frac{8\pi N}{\gamma^2\delta^2}\left\{2\sin\delta b\ \sin\delta c\ \sqrt{|p_c|} + (\sin^2\delta b + \gamma^2\delta^2)\frac{p_b\ \mathrm{sgn}(p_c)}{\sqrt{|p_c|}}\right\},
\end{aligned} \tag{2}
$$

where the holonomies in the directions r, θ, ϕ, integrated along curves of length δ, are

$$
h_1 = \cos\frac{\delta c}{2} + 2\tau_3\sin\frac{\delta c}{2}, \qquad h_2 = \cos\frac{\delta b}{2} - 2\tau_1\sin\frac{\delta b}{2}, \qquad h_3 = \cos\frac{\delta b}{2} + 2\tau_2\sin\frac{\delta b}{2}, \tag{3}
$$

and $V = 4\pi\sqrt{|p_c|}p_b$ is the spatial section volume.

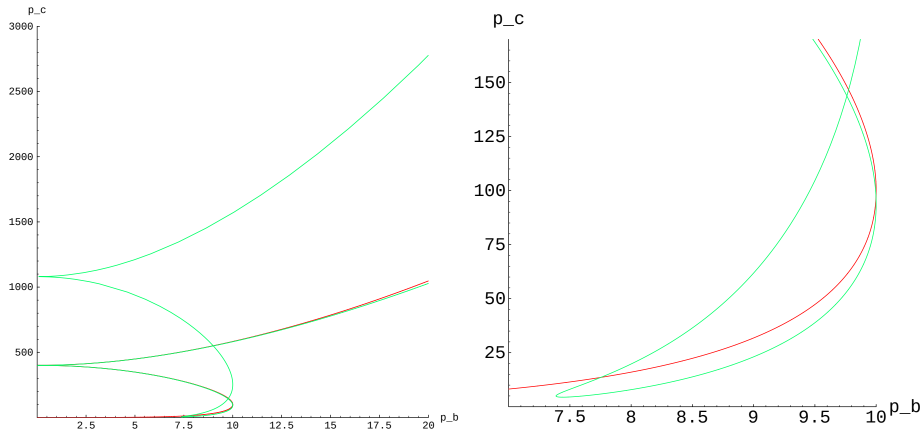

Figure 1: Semiclassical dynamical trajectory in the plane $p_b - p_c$. The plots for $p_c > 0$ and for $p_c < 0$ are disconnected and symmetric but we plot only the positive values of p_c. The red trajectory corresponds to the classical Schwarzschild solution and the green trajectory corresponds to the semiclassical solution. The plot on the right represents a zoom of trajectory region where the semiclassical analysis becomes relevant.

From (4) we obtain two independent sets of equations of motion on the phase space

$$
\begin{aligned}
&\dot{c} = -2\sin\delta c, && \dot{p_c} = 2\delta p_c \cos\delta c \\
&\dot{b} = -\Big(\sin\delta b + \frac{\gamma^2\delta^2}{\sin\delta b}\Big), && \dot{p_b} = \delta\, \cos\delta b\Big(1 - \frac{\gamma^2\delta^2}{\sin^2\delta b}\Big) p_b.
\end{aligned}
\tag{5}
$$

Solving the first three equations and using the Hamiltonian constraint $\mathcal{C}^\delta = 0$ we obtain [17]

$$
\begin{aligned}
& c(t) = \frac{2}{\delta}\arctan\Big(\mp\frac{\gamma\delta m p_b^{(0)}}{2t^2}\Big), \\
& p_c(t) = \pm\frac{1}{t^2}\Big[\Big(\frac{\gamma\delta m p_b^{(0)}}{2}\Big)^2 + t^4\Big] \\
, \quad & \cos\delta b = \sqrt{1+\gamma^2\delta^2}\left[\frac{\sqrt{1+\gamma^2\delta^2} + 1 - \left(\frac{2m}{t}\right)^{\sqrt{1+\gamma^2\delta^2}}(\sqrt{1+\gamma^2\delta^2} - 1)}{\sqrt{1+\gamma^2\delta^2} + 1 + \left(\frac{2m}{t}\right)^{\sqrt{1+\gamma^2\delta^2}}(\sqrt{1+\gamma^2\delta^2} - 1)}\right], \\
& p_b(t) = -\frac{2\,\sin\delta c\,\sin\delta b\, p_c}{\sin^2\delta b + \gamma^2\delta^2},
\end{aligned}
\tag{6}
$$

(we have used the parametrization $t \equiv e^{\delta T}$ [17]). Respect to the classical Schwarzschild solution p_c has an absolute minimum in $t_{min} = (\gamma\delta m p_b^{(0)}/2)^{1/2}$, and $p_c(t_{min}) = \gamma\delta m p_b^{(0)} > 0$. The solution presents an inner horizon in [17]

$$
t^* = 2m\left(\frac{\sqrt{1+\gamma^2\delta^2} - 1}{\sqrt{1+\gamma^2\delta^2} + 1}\right)^{\frac{2}{\sqrt{1+\gamma^2\delta^2}}}. \tag{7}
$$

We study the trajectory in the plane $p_c - p_b$ and we compare the result with the Schwarzschild solution. In Fig.1 we have a parametric plot of p_c and p_b for $m = 10$ and $\gamma\delta \sim 1$ to amplify the

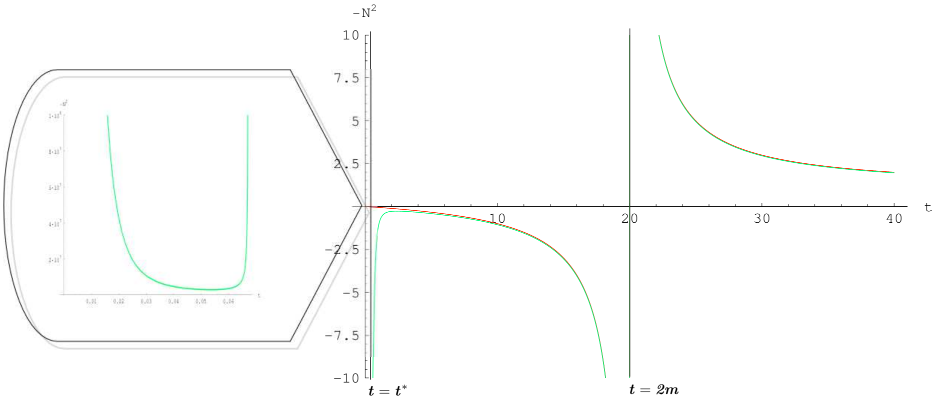

Figure 2: Plot of the lapse function $-N^2(t)$ for $m = 10$ and $\gamma\delta \sim 1$ (in the horizontal axis we have the temporal coordinate t and in the vertical axis the lapse function). The red trajectory corresponds to the classical Schwarzschild solution inside the event horizon and the green trajectory corresponds to the semiclassical solution. In the left side we have a zoom of $-N^2(t)$ in the region $0 \leqslant t \leqslant t^*$.

quantum gravity effects in the plot (in [17] it has been showed that $\delta \sim 10^{-33}$ [2] ; if we introduce a characteristic size length L for the system under consideration we can set $\delta = l_P/L$). In Fig.1 we can follow the trajectory from $t > 2m$ where the classical (red trajectory) and the semiclassical (green trajectory) solution are very close. For $t = 2m$, $p_c \to (2m)^2$ and $p_b \to 0$ (this point corresponds to the Schwarzschild radius). From this point decreasing t we reach a minimum value for $p_{c,m} \equiv p_c(t_{min}) > 0$. From $t = t_{min}$, p_c starts to grow again until $p_b = 0$, this point corresponds to a new horizon in $t = t^*$ localized. In the time interval $t < t_{min}$, p_c grows together with $|p_b|$ and the functions $p_c, |p_b| \to \infty$ for $t \to 0$; in particular $|p_b| \sim t^{-\sqrt{1+\gamma^2\delta^2}}$ for $t \sim 0$.

Metric form of the solution. In this paragraph we present the metric form of the solution. The Kantowski-Sachs metric is $ds^2 = -N^2(t)dt^2 + X^2(t)dr^2 + Y^2(t)(d\theta^2 + \sin\theta d\phi^2)$ and the metric components are related to the connection variables by

$$Y^2(t) = |p_c(t)|, \quad X^2(t) = \frac{p_b^2(t)}{|p_c(t)|}, \quad N^2(t) = \frac{\gamma^2\delta^2|p_c(t)|}{t^2\sin^2\delta b}. \tag{8}$$

The explicit form of the lapse function $N(t)^2$ in terms of the temporal coordinate t is

$$N^2(t) = \frac{\gamma^2\delta^2\left[\left(\frac{\gamma\delta m}{2t^2}\right)^2 + 1\right]}{1 - (1+\gamma^2\delta^2)\left[\frac{\sqrt{1+\gamma^2\delta^2}+1-\left(\frac{2m}{t}\right)^{\sqrt{1+\gamma^2\delta^2}}(\sqrt{1+\gamma^2\delta^2}-1)}{\sqrt{1+\gamma^2\delta^2}+1+\left(\frac{2m}{t}\right)^{\sqrt{1+\gamma^2\delta^2}}(\sqrt{1+\gamma^2\delta^2}-1)}\right]^2}. \tag{9}$$

In Fig.2 we have a plot of the lapse function $-N(t)^2$ ($\forall t \geqslant 0$), for $m = 10$ and $\gamma\delta \sim 1$ (we have taken $\gamma\delta \sim 1$ to amplify, in the plot, the loop quantum gravity modifications at the Planck scale). The red

[2]The parameter δ is related to the minimum area eigenvalue that in quantum geometry is $\sim l_P^2$ [18].

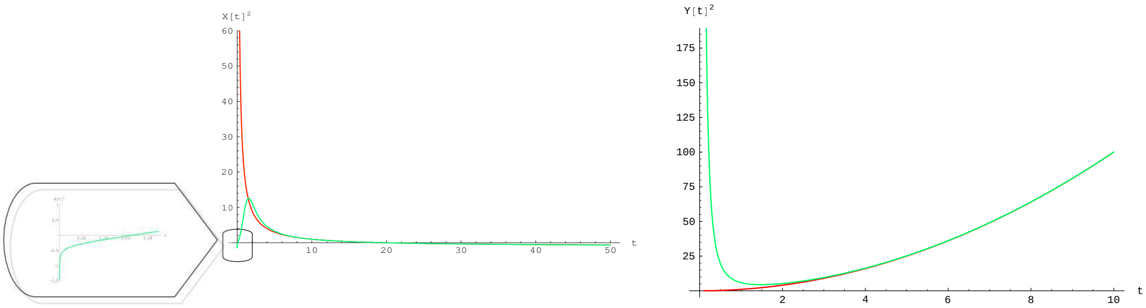

Figure 3: Plot of $X^2(t)$ and $Y^2(t)$ for $m = 10$, $\gamma\delta \sim 1$ and $\forall t \geqslant 0$; the event horizon for this particular values of the parameters is in $t = 20$. The red trajectory corresponds to the classical Schwarzschild solution and the green trajectory corresponds to the semiclassical solution.

trajectory corresponds to the classical solution $-1/(2m/t-1)$ and the green line to the semiclassical solution. We can observe the two solutions are identically in the space-time region far from the Planck scale. In particular they have the same asymptotic limit for $t \gg 2m$. In the region $0 \leqslant t \leqslant t^*$ a plot of $-N^2(t)$ is given in the square on the left side in Fig.2.

Using the second relation of (8) we can obtain also the other components of the metric [17],

$$X^2(t) = \frac{(2\gamma\delta m)^2 \left(1-(1+\gamma^2\delta^2)\left[\frac{\sqrt{1+\gamma^2\delta^2}+1-\left(\frac{2m}{t}\right)^{\sqrt{1+\gamma^2\delta^2}}(\sqrt{1+\gamma^2\delta^2}-1)}{\sqrt{1+\gamma^2\delta^2}+1+\left(\frac{2m}{t}\right)^{\sqrt{1+\gamma^2\delta^2}}(\sqrt{1+\gamma^2\delta^2}-1)}\right]^2\right) t^2}{(1+\gamma^2\delta^2)^2 \left(1-\left[\frac{\sqrt{1+\gamma^2\delta^2}+1-\left(\frac{2m}{t}\right)^{\sqrt{1+\gamma^2\delta^2}}(\sqrt{1+\gamma^2\delta^2}-1)}{\sqrt{1+\gamma^2\delta^2}+1+\left(\frac{2m}{t}\right)^{\sqrt{1+\gamma^2\delta^2}}(\sqrt{1+\gamma^2\delta^2}-1)}\right]^2\right)^2 \left[\left(\frac{\gamma\delta m}{2}\right)^2+t^4\right]}. \tag{10}$$

and the radius of the S^2 sphere as a function of the temporal coordinate is

$$Y^2(t) = \frac{1}{t^2}\left[\left(\frac{\gamma\delta m}{2}\right)^2 + t^4\right]. \tag{11}$$

In Fig.3 a plot of $X^2(t)$ inside and outside the event horizon, $\forall t \geqslant 0$ is represented. From the solution (10) we can calculate the limit for $t \to 0$ and for $t \to \infty$ and we obtain $X^2(t \to 0) \to -\infty$ ($X^2(t) \sim t^{-\gamma^2\delta^2}$ for $t \sim 0$) and $X^2(t \to \infty) \to -1$ (the large distance limit is $X^2(t) \sim -1 + \gamma^2\delta^2 \ln \frac{2m}{t}$, but the logarithmic correction is meaningful for a distance $t \sim e^{1/\delta^2}$ which is longer the universe radius). The value of the coordinate t where the solution $X^2(t)$ changes sign corresponds to the inner horizon in $t = t^*$ localized. In the second picture of Fig.3 we have a plot of $Y^2(t)$ and we can note a substantial difference with the classical solution. In the classical case the S^2 sphere goes to zero for $t \to 0$. In the semiclassical solution instead the S^2 sphare bounces on a minimum value of the radius, which is $Y^2(t_{min}) = \gamma\delta m$, and it expands again to infinity for $t \to 0$. The minimum of $Y^2(t)$ corresponds to the time coordinate $t_{min} = (m\gamma\delta/2)^{1/2}$.

It is useful make a change in variables from $t \to r$ in order to study the evaporation process, and we focus our attention on the outside event horizon region toward the near horizon region. From the outside event horizon point of view the causal structure of the space-time is defined by the identifications $-N^2(t) \to g_{rr}(r)$ and $X^2(t) \to g_{tt}(r)$. We redefine also the S^2 sphere radius in terms of metric components, $Y^2(t) \to Y^2(r) = g_{\theta\theta}(r) = g_{\phi\phi}/\sin^2\theta$. The solution can be summarized in the following table.

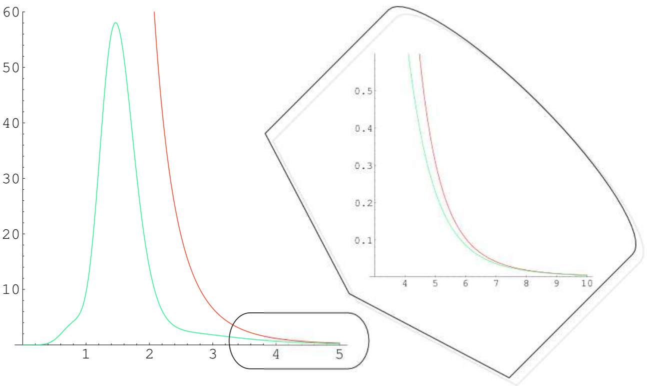

Figure 4: Plot of the invariant $\mathrm{R}_{\mu\nu\rho\sigma}\mathrm{R}^{\mu\nu\rho\sigma}$ for $m = 10$, $\gamma\delta \sim 1$ and $\forall t \geqslant 0$; the large t behaviour is $1/t^6$ as shown in the zoom on the right side.

$g_{\mu\nu}$	Semiclassical	Classical
$g_{tt}(r)$	$\dfrac{(2\gamma\delta m)^2\left(1-(1+\gamma^2\delta^2)\left[\frac{\sqrt{1+\gamma^2\delta^2}+1-\left(\frac{2m}{r}\right)^{\sqrt{1+\gamma^2\delta^2}}(\sqrt{1+\gamma^2\delta^2}-1)}{\sqrt{1+\gamma^2\delta^2}+1+\left(\frac{2m}{r}\right)^{\sqrt{1+\gamma^2\delta^2}}(\sqrt{1+\gamma^2\delta^2}-1)}\right]^2\right)}{(1+\gamma^2\delta^2)^2\left(1-\left[\frac{\sqrt{1+\gamma^2\delta^2}+1-\left(\frac{2m}{r}\right)^{\sqrt{1+\gamma^2\delta^2}}(\sqrt{1+\gamma^2\delta^2}-1)}{\sqrt{1+\gamma^2\delta^2}+1+\left(\frac{2m}{r}\right)^{\sqrt{1+\gamma^2\delta^2}}(\sqrt{1+\gamma^2\delta^2}-1)}\right]^2\right)^2\left[\left(\frac{\gamma\delta m}{2r}\right)^2+r^2\right]}$	$-(1-\frac{2m}{r})$
$g_{rr}(r)$	$-\dfrac{\gamma^2\delta^2\left[\left(\frac{\gamma\delta m}{2r^2}\right)^2+1\right]}{1-(1+\gamma^2\delta^2)\left[\frac{\sqrt{1+\gamma^2\delta^2}+1-\left(\frac{2m}{r}\right)^{\sqrt{1+\gamma^2\delta^2}}(\sqrt{1+\gamma^2\delta^2}-1)}{\sqrt{1+\gamma^2\delta^2}+1+\left(\frac{2m}{r}\right)^{\sqrt{1+\gamma^2\delta^2}}(\sqrt{1+\gamma^2\delta^2}-1)}\right]^2}$	$\frac{1}{1-\frac{2m}{r}}$
$g_{\theta\theta}(r) = \frac{g_{\phi\phi}(r)}{\sin^2\theta}$	$\left(\frac{\gamma\delta m}{2r}\right)^2 + r^2$	r^2

If we develop the metric in the table by the parameter δ (or l_P in dimensionless units) we obtain the Schwarzschild solution to zero order: $g_{tt}(r) = -(1-2m/r) + O(\delta^2)$, $g_{rr}(r) = 1/(1-2m/r) + O(\delta^2)$ and $g_{\theta\theta}(r) = g_{\phi\phi}(r)/\sin^2\theta = r^2 + O(\delta^2)$.

Regular semiclassical solution in $r = 0$. In this paragraph we show the semiclassical solution is regular in $r = 0$ where the classical singularity is localized. We calculate the curvature invariant $\mathrm{R}_{\mu\nu\rho\sigma}\mathrm{R}^{\mu\nu\rho\sigma}$ and we plot the result in terms of the variable t. The classical singularity is in $t = 0$ localized. We express the curvature invariant in terms of the functions $N(t)$, $X(t)$ and $Y(t)$ of the previous section and we obtain

$$\begin{aligned}\mathrm{R}_{\mu\nu\rho\sigma}\mathrm{R}^{\mu\nu\rho\sigma} = 4\Bigg[&\left(\frac{1}{XN}\frac{d}{dt}\left(\frac{1}{N}\frac{dX}{dt}\right)\right)^2 + 2\left(\frac{1}{YN}\frac{d}{dt}\left(\frac{1}{N}\frac{dY}{dt}\right)\right)^2 + \\ &+2\left(\frac{1}{XN}\frac{dX}{dt}\frac{1}{YN}\frac{dY}{dt}\right)^2 + \frac{1}{Y^4N^4}\left(N^2+\left(\frac{dY}{dt}\right)^2\right)^2\Bigg].\end{aligned} \tag{12}$$

Introducing the explicit form of the metric in (12) we obtain a regular quantity in $t = 0$.We give in Fig.4 a plot of the result in term of the coordinate t. From the plot it is evident that the curvature

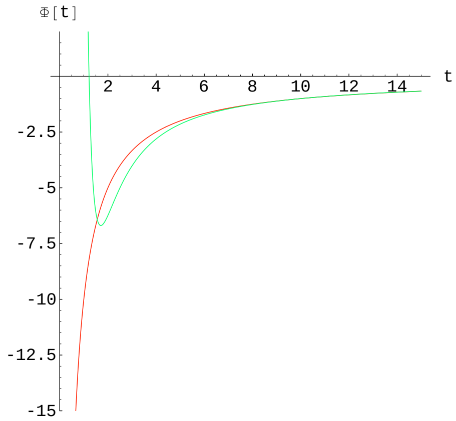

Figure 5: Plot of the first correction to the gravitational potential for $m = 10$ and $\gamma\delta \sim 1$ to amplify the quantum gravity effects; the red trajectory corresponds to the classical potential and the green trajectory to the semiclassical one.

invariant tends to zero for $t \to 0$ and match with the classical quantity for large value of the time coordinate t. We give below the first correction in δ to the curvature invariant

$$\begin{aligned} \mathrm{R}_{\mu\nu\rho\sigma}\mathrm{R}^{\mu\nu\rho\sigma} &= \frac{48\mathrm{m}^2}{\mathrm{t}^6} \\ &+ \frac{8m\gamma^2\delta^2}{t^{10}}\left(-33m^3 + 12m^2 t - 6m^2 t^3 + 2t^5 + 2mt^4(\ln(8) - 1) + 6mt^4 \ln\left(\frac{m}{t}\right)\right) + O(\delta^3). \end{aligned} \quad (13)$$

From (13) we can see that the first correction to the curvature invariant is singular in $t = 0$ and this is the same for each other orders. This note shows that the regularity of the semiclassical solution is a genuinely non perturbative result. (For the semiclassical solution the trace of the Ricci tensor ($\mathrm{R} = \mathrm{R}^{\mu}_{\mu}$) is not identically zero as for the Schwarzschild solution. We have calculated the trace invariant and we have showed that also this quantity is regular in $r = 0$).

Corrections to the Newtonian potential. Another quantity that we can extract from the semiclassical metric is the first correction of gravitational potential. The gravitational potential is related to the metric by $\Phi(r) = -\frac{1}{2}(g_{tt}(r) + 1)$. Developing the metric component (10) by the parameter δ we obtain the first correction to the gravitational potential

$$\Phi(r) = -\frac{m}{r} - \frac{\gamma^2\delta^2}{2}\left(1 + \ln\left(\frac{2m}{r}\right) - \frac{m}{r}\ln\left(\frac{2m}{r}\right) - \frac{3m}{r} + \frac{2m^2}{r^2} + \frac{m^2}{4r^4} - \frac{m^3}{2r^5}\right). \quad (14)$$

The parameter $\delta = l_P/L$, where L is the characteristic length of the physical system, plays the role of dimensionless Plank length. When we restore the length units the first five terms are multiplied by $(l_P/L)^2$ and the last two by l_P^2.

2 Temperature, entropy and evaporation

The form of the metric calculated in the preview section and in [17] has the general form

$$ds^2 = -g(r)dt^2 + f^{-1}(r)dr^2 + h^2(r)(d\theta^2 + \sin^2\theta d\phi^2), \quad (15)$$

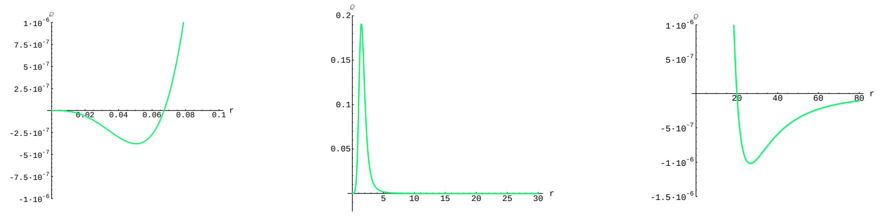

Figure 6: Plot of the effective energy density ρ for $m = 10$ and $\gamma\delta \sim 1$. The plots represent the energy density (in the center plot) and two zooms for $r \sim 0$ and $r \gtrsim 2m$.

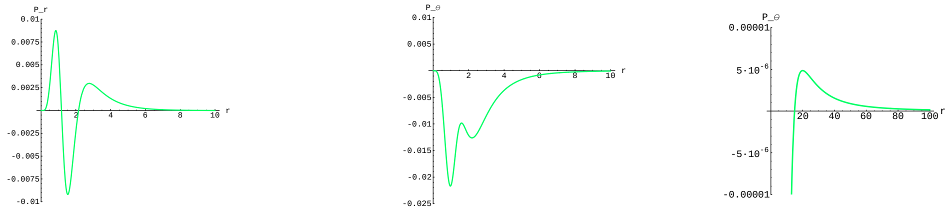

Figure 7: Plot of the pressures P_r, P_θ for $m = 10$ and $\gamma\delta \sim 1$. The first plot represents the pressure P_r, the second and the third plot represent the pressure P_θ for $r \leqslant 2m$ and $r \gtrsim 2m$ respectively.

where the functions $f(r)$, $g(r)$ and $h(r)$ depend on the mass parameter m and are given in the table of the first section. We can introduce the null coordinate v to express the metric (15) in the Bardeen form. The null coordinate v is defined by the relation $v = t + r^*$, where $r^* = \int^r dr/\sqrt{f(r)g(r)}$ and the differential is $dv = dt + dr/\sqrt{f(r)g(r)}$. In the new coordinate the metric is

$$ds^2 = -g(r)dv^2 + 2\sqrt{\frac{g(r)}{f(r)}}\, drdv + h^2(r)(d\theta^2 + \sin^2\theta d\phi^2). \tag{16}$$

We can interpret our black hole solution has been generated by an effective matter fluid that simulates the loop quantum gravity corrections (in analogy with the paper [19]). The effective gravity-matter system satisfies by definition of the Einstein equation $\mathbf{G} = 8\pi\mathbf{T}$, where $\mathbf{T}$ is the effective energy tensor. In this paper we are not interested to the explicit form of the stress energy tensor however we give a plot of the tensor components for completeness. It is possible to calculate the stress energy tensor by using the Einstein equations. The stress energy tensor for a perfect fluid compatible with the space-time symmetries is $T^\mu_\nu = (-\rho, P_r, P_\theta, P_\theta)$ and in terms of the Einstein tensor the components are $\rho = -G^t_t/8\pi G_N$, $P_r = G^r_r/8\pi G_N$ and $P_\theta = G^\theta_\theta/8\pi G_N$. We can calculate the Einstein tensor components using the metric in the table of section one. The components of the effective energy tensor that simulates quantum gravity effects are plotted in Fig.6 and Fig.7. In the plots we have amplified quantum gravity effects taking $\gamma\delta \sim 1$, however it is evident that the energy density and pressure are meaningful only in the Planck region. In the contrary for $r \gg l_P$, energy density and pressure tend to zero. To the second order in δ^2 the energy density is

$$\rho = \frac{m(7m^2 - r^4 + mr(2r^2 - 3))\gamma^2\delta^2}{8\pi G_N\, r^7}. \tag{17}$$

If we develop the semiclassical metric solution of section one to order δ^2 and we introduce the result in the Einstein tensor G^μ_ν, we obtain (to order δ^2) the energy density (17). The semiclassical metric to zero order in δ is the classical Schwarzschild solution ($g^C_{\mu\nu}$) and $G^\mu_\nu(g^C) \equiv 0$.

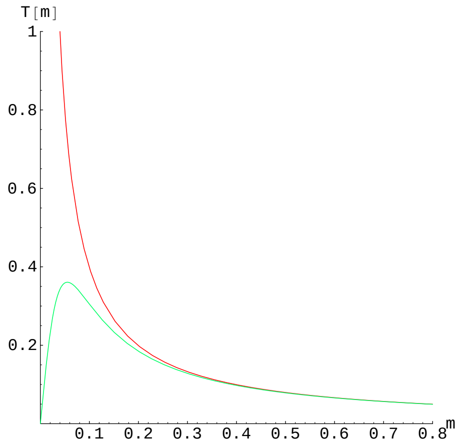

Figure 8: Plot of the temperature as function of the mass m and $\gamma\delta \sim 1$ to amplify the quantum gravity effects; the red trajectory corresponds to the Hawking temperature $T_H = 1/8\pi m$ and the green trajectory corresponds to the quantum geometry temperature.

Temperature. In this paragraph we are interested in calculate the temperature and entropy for our modified black hole solution and analyze the evaporation process. The Bekenstein-Hawking temperature is given in terms of the surface gravity κ by $T_{BH} = \kappa/2\pi$. The surface gravity is defined by

$$\kappa^2 = -\frac{1}{2} g^{\mu\nu} g_{\rho\sigma} \nabla_\mu \chi^\rho \nabla_\nu \chi^\sigma = -\frac{1}{2} g^{\mu\nu} g_{\rho\sigma} \Gamma^\rho_{\mu 0} \Gamma^\sigma_{\nu 0}, \tag{18}$$

where $\chi^\mu = (1,0,0,0)$ is a timelike Killing vector and $\Gamma^\mu_{\nu\rho}$ is the connection compatibles with the metric $g_{\mu\nu}$ of (15). Using the semiclassical metric in the table of section one we can calculate the surface gravity in $r = 2m$ obtaining $\kappa^2 = -\frac{1}{4} g^{00} g^{11} \left(\frac{\partial g_{00}}{\partial r}\right)^2 = \left(\frac{16m}{64m^2+\gamma^2\delta^2}\right)^2$, therefore the temperature is

$$T_{BH} = \frac{8m}{\pi(64m^2 + \gamma^2\delta^2)}. \tag{19}$$

The temperature in (19) coincides with the Hawking temperature in the limit $\delta \to 0$. In Fig.8 we have a plot of the temperature as a function of the black hole mass m. The red trajectory corresponds to the Hawking temperature and the green trajectory corresponds to the semiclassical one. There is a substantial difference for small values of the mass, in fact the semiclassical temperature tends to zero and does not diverge for $m \to 0$. The temperature is maximum for $m = \gamma\delta/8$ and $T_{\max} = 1/2\pi\gamma\delta$.

Entropy. Another interesting quantity to calculate is the entropy and its quantum corrections. By definition $S_{BH} = \int dm/T_{BH}(m)$ and we obtain

$$S_{BH} = 4\pi m^2 + \frac{\gamma^2\delta^2}{16} \ln m^2. \tag{20}$$

On the other hand the event horizon area (in $r = 2m$) is

$$A = \int d\phi d\theta \sin\theta \, Y^2(r) = 16\pi m^2 + \frac{\pi\gamma^2\delta^2}{4}. \tag{21}$$

Using (21) we can express the entropy in terms of the event horizon area

$$
\begin{aligned}
S_{BH} &= \frac{A}{4} + \frac{\gamma^2\delta^2}{16}\ln\left[\frac{A}{4}\left(1-\frac{\pi\gamma^2\delta^2}{4A}\right)\right] - \frac{\pi\gamma^2\delta^2}{16} - \frac{\gamma^2\delta^2}{16}\ln 4\pi = \\
&= \frac{A}{4} + \frac{\gamma^2\delta^2}{16}\ln\left(\frac{A}{4}\right) + \frac{\gamma^2\delta^2}{16}\ln\left(1-\frac{\pi\gamma^2\delta^2}{4A}\right) - \frac{\pi\gamma^2\delta^2}{16} - \frac{\gamma^2\delta^2}{16}\ln 4\pi = \\
&= \frac{A}{4} + \frac{\gamma^2\delta^2}{16}\ln\left(\frac{A}{4}\right) - \frac{\gamma^2\delta^2}{16}\sum_{n=1}^{\infty}\frac{1}{n}\left(\frac{\pi\gamma^2\delta^2}{4A}\right)^n - \frac{\pi\gamma^2\delta^2}{16} - \frac{\gamma^2\delta^2}{16}\ln 4\pi. \qquad (22)
\end{aligned}
$$

In the last step we have developed the second ln-function for $\delta^2 \ll A$ to compare our result with the general formula in letterature $S = \frac{A}{4} + \rho\ln\left(\frac{A}{4}\right) + \sum_{n=1} c_n \left(\frac{4}{A}\right)^n + const.$. Our calculation reproduces the standard area term and the logarithmic correction. In (22) the $(\delta^2/A)^n$ corrections appear in the form of another logarithmic function.

Evaporation process. In the previews paragraph the metric (16) is a static solution of the effective Einstein equation of motion outside the event horizon. That solution is a right even if the mass is a function of the null coordinate v but with a non static effective stress energy tensor. In this paper we are not interested in the explicit form of the energy tensor. Instead we are interested in the evaporation process of the mass and in particular in the energy flux from the black hole. The luminosity can be estimated using the Stefan law and it is given by $\mathcal{L}(m) = \sigma A(m) T_{BH}^2(m)$, where (for a single massless field with two degree of freedom) $\sigma = \pi^2/60$, $A(m)$ is the event horizon area and $T_{BH}(m)$ is the Bekenstein-Hawking temperature calculated in the previous section. At the first order in the luminosity the metric (16) witch incorporates the decreasing mass as function of the null coordinate v is also a solution but with a new effective stress energy tensor as underlined previously. Introducing the results (19) and (21) of the previous paragraph in the luminosity $\mathcal{L}$ we obtain

$$
\mathcal{L}(m) = \frac{2^{16}m^6 + 2^{10}\gamma^2\delta^2 m^4}{60\pi(64m^2+\gamma^2\delta^2)^4}. \qquad (23)
$$

Using (23) we can solve the fist order differential equation

$$
-\frac{dm(v)}{dv} = \mathcal{L}[m(v)] \qquad (24)
$$

to obtain the mass function $m(v)$. The result of integration with initial condition $m(v=0) = m_0$ is

$$
5120\pi(m-m_0)^3 + 720\pi\gamma^2\delta^2(m-m_0) - \frac{45\pi\gamma^4\delta^4}{4}\left(\frac{1}{m}-\frac{1}{m_0}\right) - \frac{5\pi\gamma^6\delta^6}{256}\left(\frac{1}{m^3}-\frac{1}{m_0^3}\right) = -v. \qquad (25)
$$

In Fig.9 there is an implicit plot of $m(v)$ and it is evident the difference with the classical result. Classically (red trajectory) the mass evaporates in a finite time but at the semiclassical level (green trajectory) the mass evaporates in an infinite time. We can calculate the value of m where the concavity of $m(v)$ changes. From the second derivative of the function $m(v)$ we obtain

$$
\frac{d^2m(v)}{dv^2} \sim -\mathcal{L}[m(v)]\frac{1024m^3(32m^2-\gamma^2\delta^2)}{15\pi(64m^2+\gamma^2\delta^2)^4}. \qquad (26)
$$

and equalling (26) to zero we obtain the mass $m_c = \frac{\gamma\delta}{4\sqrt{2}}$. The value m_c is in the order Planck mass and at this scale it is inevitable a complete quantum analysis of the problem. However in this semiclassical study the evaporation process needs of infinite time.

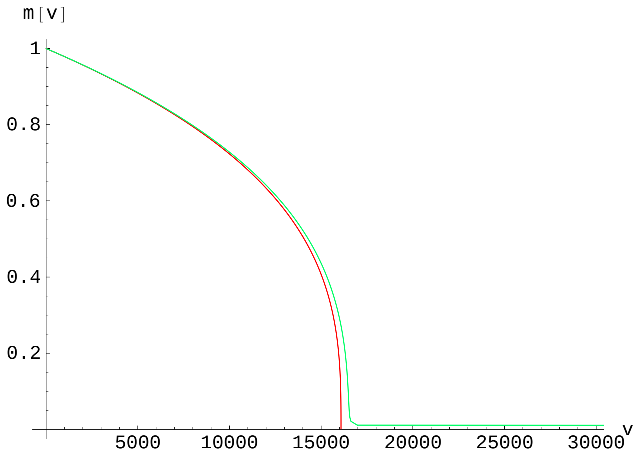

Figure 9: Plot of $m(v)$ for $m_0 = 1$, $\gamma\delta \sim 1$ and $\forall v \geqslant 0$. In the plot it is evident that classically (red trajectory) the mass evaporate in a finite time, on the contrary using the solution suggested by loop quantum black hole the mass evaporate in an infinite time.

Conclusions

In this paper we have extended to all space time the regular solution calculated and studied inside the event horizon in the preview paper [17]. The solution has been obtained solving the Hamilton equation of motion for the Kantowski-Sachs space-time [20] using the regularized Hamiltonian constraint suggested by loop quantum gravity. The semiclassical solution reproduces the Schwarzschild solution at large distance from the event horizon but it is substantially different in the Planck region near the point $r = 0$, where the singularity is (classically) localized. The solution has two event horizons : the first in $r = 2m$ and the other near the point $r = 0$ (this suggests a similarity with the result in "asymptotic safety quantum gravity" [19], but the radius of such horizon is smaller than the Planck length and in this region it is inevitable a complete quantum analysis of the problem [16]).

In this paper we have concentrated our attention on the evaporation process and we have calculated the temperature, entropy (with all the correction suggested by the particular model) and the mass variation formula as seen by a distant observer at the time v. The main results are:

1. The classical black hole singularity near $r \sim 0$ disappears from the semiclassical solution. The classical divergent curvature invariant is bounded in the the semiclassical theory and in particular $\mathrm{R}_{\mu\nu\rho\sigma}\,\mathrm{R}^{\mu\nu\rho\sigma} \to 0$ for $r \to 0$ and for $r \to \infty$.

2. The Bekenstein-Hawking temperature $T_{BH}(m)$ is regular for $m \sim 0$ and tends to zero

$$T_{BH} = \frac{8m}{\pi(64m^2 + \gamma^2\delta^2)}. \tag{27}$$

3. The black hole entropy in terms of the horizon area reproduces the $A/4l_P^2$ term but contain also the ln-correction and all the other correction in $(l_P^2/A)^n$

$$S = \frac{A}{4l_P^2} + \frac{\gamma^2}{16}\ln\left(\frac{A}{4l_P^2}\right) + \frac{\gamma^2}{16}\ln\left(1 - \frac{4\pi\gamma^2 l_P^2}{16A}\right) + \mathrm{const}, \tag{28}$$

(where we have repristed the length units).

4. The evaporation process needs an infinite time in our semiclassical analysis but the difference with the classical result is evident only at the Planck scale when the black hole mass is the order $m \sim m_c = \gamma\delta/4\sqrt{2}$. In this extreme energy conditions it is inevitable a complete quantum gravity analysis that can implies a complete evaporation [22].

We think that the semiclassical analysis performed here will sheds light on the problem of the "information loss" in the process of black hole formation and evaporation but a complete quantum analysis is necessary to understand what happen in the Planck region. See in particular [22] for a possible physical interpretation of the black hole information loss problem.

Acknowledgements

We are strongly indebted to Roberto Balbinot for crucial criticisms, inputs and suggestions. We are grateful also to Alfio Boananno, Eugenio Bianchi and Guido Cossu for many important and clarifying discussion.

References

[1] Carlo Rovelli, *Quantum Gravity*, (Cambridge University Press, Cambridge, 2004); A. Ashtekar, *Background independent quantum gravity: A Status report*, Class. Quant. Grav. 21, R53 (2004), gr-qc/0404018; T. Thiemann, *Loop quantum gravity: an inside view*, hep-th/0608210; T. Thiemann, *Introduction to Modern Canonical Quantum General Relativity*, gr -qc/0110034; *Lectures on Loop Quantum Gravity*, Lect. Notes Phys. 631, 41-135 (2003), gr-qc/0210094

[2] Martin Reuter, *Non perturbative evolution equation for quantum gravity*, Phys. Rev. D57 971-985 (1998), hep-th/9605030

[3] F. Conrady, L. Doplicher, R. Oeckl, C. Rovelli and M. Testa *Minkowski vacuum in background independent quantum gravity*, Phys. Rev. D 69 064019, gr-qc/0307118; Daniele Colosi, Luisa Doplicher, Winston Fairbairn, Leonardo Modesto, Karim Noui and Carlo Rovelli, *Background independence in a nutshell: dynamics of a tetrahedron*, Class. Quant. Grav. 22 (2005) 2971-2989, gr-qc/0408079

[4] Leonardo Modesto and Carlo Rovelli, *Particle scattering in loop quantum gravity*, Phys. Rev. Lett. 95 191301 (2005), gr-qc/0502036

[5] Carlo Rovelli, *Graviton propagator from background-independent quantum gravity*,Phys. Rev. Lett. 97 151301 (2006), gr-qc/0508124

[6] Eugenio Bianchi, Leonardo Modesto, Carlo Rovelli and Simone Speziale, *Graviton propagator in loop quantum gravity*, Class. Quant. Grav. 23 (2006) 6989 -7028, gr-qc/0604044

[7] Simone Speziale, *Towards the graviton from spinfoams : the 3D toy model*, J. high Energy Phys. JHEP05 (2006) 039, gr-qc/0512102

[8] E. Livine and S. Speziale, *Group integral techniques for the spinfoam graviton propagator*, gr-qc/0608131

[9] Laurent Freidel and Etera R. Livine *Ponzano-Regge model revisited III: Feynman diagrams and effective field theory*, Class. Quant. Grav. 23 2021-2062 (2006), hep-th/0502106

[10] Aristide Baratin and Laurent Freidel, *Hidden quantum gravity in 4d Feynman diagrams: emergence of spin foams*, hep-th/0611042

[11] M. Bojowald, *Inverse scale factor in isotropic quantum geometry*, Phys. Rev. D64 084018 (2001); M. Bojowald, *Loop Quantum Cosmology IV: discrete time evolution*, Class. Quant. Grav. 18, 1071 (2001); Martin Bojowald, "Loop quantum cosmology: recent progress", gr-qc/0402053

[12] A. Ashtekar, M. Bojowald and J. Lewandowski, *Mathematica structure of loop quantum cosmology*, Adv. Theor. Math. Phys. 7 (2003) 233-268, gr-qc/0304074

[13] Leonardo Modesto, *Disappearance of the black hole singularity in loop quantum gravity*, Phys. Rev. D 70 (2004) 124009, gr-qc/0407097

[14] Leonardo Modesto, *The kantowski-Sachs space-time in loop quantum gravity*, International Journal of Theoretical Physics, published on line 1 june 2006, gr-qc/0411032

[15] Leonardo Modesto, *Gravitational collapse in loop quantum gravity*, gr-qc/0610074; Leonardo Modesto, *Quantum gravitational collapse*, gr-qc/0504043

[16] A. Ashtekar and M. Bojowald, *Quantum geometry and Schwarzschild singularity* Class. Quant. Grav. 23 (2006) 391-411, gr-qc/0509075; Leonardo Modesto, *Loop quantum black hole*, Class. Quant. Grav. 23 (2006) 5587-5602, gr-qc/0509078

[17] Leonardo Modesto, Black hole interior from loop quantum gravity, gr-qc/06011043;

[18] C. Rovelli and L. Smolin, "Loop Space Representation Of Quantum General Relativity," Nucl. Phys. B 331 (1990) 80; C. Rovelli and L. Smolin, "Discreteness of area and volume in quantum gravity," Nucl. Phys. B 442 (1995) 593

[19] Alfio Bonanno, Martin Reuter, *Renormalization group improved black hole space-times*, Phys. Rev. D 62 (2000) 043008, hep-th/0002196; Alfio Bonanno, Martin Reuter *Spacetime structure of an evaporating black hole in quantum gravity*, Phys. Rev. D 73 (2006) 083005, hep-th/0602159

[20] R. Kantowski and R. K. Sachs, J. Math. Phys. 7 (3) (1966)

[21] Abhay Ashtekar, *New Hamiltonian formulation of general relativity*, Phys. Rev. D 36 1587-1602

[22] Abhay Ashtekar & Martin Bojowald, *Black hole evaporation : A paradigm* Class. Quant. Grav. 22 (2005) 3349-3362, gr-qc/0504029